IJCRT.ORG ISSN : 2320-2882

INTERNATIONAL JOURNAL OF CREATIVE RESEARCH THOUGHTS (IJCRT)

An International Open Access, Peer-reviewed, Refereed Journal

Automatic Segmentation for Acute Leukemia Cells from Peripheral Blood Smear Images

Najaat A. A. Abdullah[1], Mohammed A. M. Ibrahim[2], Adel S. M. Haider[3]

[1] *Department of Information Technology, Faculty of Engineering, Aden University, Yemen,*

[2] *Department of Information Technology, Faculty of Engineering, Taiz University, Yemen,*

[3] *Department of Information Technology, Faculty of Engineering, Aden University, Yemen,*

Corresponding Author: Najaat A. A. Abdullah

Abstract

Leukemia is a type of malignancy blood cancer occurring in both adults and children due to a rapid development of abnormal white blood cells. In the diagnostic process, abnormal white blood cells (blast cells) play an important role for hematologists. Whereas the treatment is usually allocated based on the leukemia types and subtypes which depending upon the morphological features of the cell under microscope. Thus, the blast cells segmentation is the first step for diagnostic process. Generally, this paper aims to develop a methodology to detect and localize acute leukemia blast cells based on image processing techniques using peripheral blood smear images. To achieve this aim, the blast cells were localized by removing other blood components and then the region of interest was segmented into sub-images. The problem of overlapped cells was also addressed for better classification. This stage was accomplished by using various image processing techniques such as; color transformation, threshold algorithm, mathematical morphological operations, and watershed segmentation. The k-means clustering and mathematical subtraction operation were used to further segment the blast cell into its nucleus and cytoplasm, respectively. Based on the Image Segmentation Quality Scores, the proposed algorithm in this study was able to segment the blast cell region and its nucleus with a high level of accuracy of 97% and 94%, respectively. The proposed segmentation algorithm achieved an overall accuracy of 96% and 93% to discriminate between acute leukemia and normal cell region and their nucleus region, respectively.

Keywords: acute leukemia, blast cells segmentation, nucleus segmentation, peripheral blood smear, segmentation evaluation

1- Introduction

Billions of new blast cells are produced and matured in the bone marrow such as white blood cells (WBCs), red blood cells (RBCs) and Platelets. They move into the bloodstream, and carry many functions like WBCs fight the infection, RBCs carry oxygen and platelets mediate blood clot. In the case of leukemia, there is an overproduction of blast cells, which have not yet been fully developed into mature cells. These cells move into the bloodstream and crowd out the normal cells and preventing them to do normal functions. Generally, leukemia is usually classified as either acute or chronic depending on how fast the cancer cells are developed. Acute leukemia can be further classified into Acute Lymphoblastic Leukemia (ALL), and Acute Myeloid Leukemia (AML). According to standard of the French American British (FAB), acute leukemia further divides into subtypes according to the cell's morphology as L1, L2 and L3 in ALL and M0, M1, M2, M3, M4, M5 and M7 in AML. Generally, many tests used to diagnosis acute leukemia such as Peripheral Blood (PB) smear examination, immunophenotyping, cytogenetic analysis, etc [1, 2]. Although the results of immunophenotyping and cytogenetic analysis tests are more accurate but do not available in all medical centers and hospitals around the world, so the PB smear examination is still considered as the best initial test of acute leukemia. The PB smear examination normally used as a follow-up test to detect the abnormal blood cells before exposing the patient to any painful examination. However, it is subjected to inter-observer differences and human errors based on their experiences.

According to these drawbacks, computer-aided diagnosis for acute leukemia based on image processing techniques avoids the error occurred by human and offer a standard diagnostic system that does not affected by the variations among observers. This system consists of a number of stages started by image segmentation which is an image processing technique to partition the image into several parts called Region of Interest (ROIs) depending on the characteristics [3]. The quality of this process is a crucial step for classification accuracy to evaluate the medical images. The purpose of this stage is to detect the blast cells and separate them from the other blood components in the PB smear images, which is considered the most difficult part in the development of the computer-aided diagnosis for acute leukemia. There are many factors made the segmentation stage is a challenging task such as; low contrast between the blast cells and its background, the presence of overlapped cells, color variation, the illumination of microscope, etc.. The implementation of the blast cells segmentation from PB smear images involved several methods such as thresholding, k-means clustering, marker control watershed, etc.

This paper is organized as follow, section 2 discusses the literature review. Section 3 describes the proposed methodology. The experimental results discussed in section 4. Finally, section 5 presents the conclusion and future work.

2- Literature Review

In order to extract a meaningful information from an image, segmentation process divides the image into various regions. However, the presence of touching or overlapping cells and staining variation limit the accuracy of feature extraction. Thus, these problems have been addressed in the literature by developing an automated systems to localize and segment WBCs from PB smear images, such as Rodellar, J. et al. [3] developed a novel segmentation scheme in order to obtain three regions of interests (ROIs) which are nucleus, entire cell and peripheral zone around the cell by utilizing the image color information and soft clustering using Gaussian mixture models of different color components. They allow to extract a new feature to distinguish abnormal cells with subtile color. The overall segmentation efficiency was 98.9%. Another attempt to detect the ROIs was achieved by Karthikeyan, T, and Poornima, N. [4] who used Fuzzy c-means clustering in order to produce a soft partition for image that contain huge sets of pixel data. In this segmentation method, the pixels can belong to more than one cluster depending on their membership. The proposed model gives satisfactory results with 90% accuracy.

In the same manner, Nelikanti, A. [5] used adaptive k-means clustering to solve the problem of different initial partitions which may lead inconsistent output for the same image. The morphological operations were performed to trace the boundaries of the cells in the image in order to detect the ROIs.

Instead of clustering algorithm, some other researchers have made a great efforts to solve the segmentation problem. For example, Rawat, J. et al. [6] proposed a technique in order to improve the discrimination process of malignant cells by separating a particular leukocyte into a single sub-image. This method discards the segmentation problems arising from overlapped cells. Thus, it may lead to misclassification of some subtypes which can be distinguished by the number of the blast cells such as; M0 and M1. When Tran, V. et al. [7] used a segmentation model based on the combination between color conversion, intensity, threshold and gradient magnitude in order to extract AML cells, the accuracy of nuclei and cytoplasm detection was 82.9%. The suggested method can also be applied to separate the cytoplasm from its background that has similar intensity. However, the method did not introduce any solution to break up the overlapped cells. Another approach to developing the segmentation process was introduced by Putzu, L. et al. [8] who used Zack algorithm to separate the nucleus and cytoplasm from isolated leukocyte using converted Y component color space. The approach achieved 92% accuracy under the same lighting and resolution conditions. However, this solution for the illumination problem may not always be valid for the diagnostic process because the PB smear images can be taken under varying lighting conditions.

While Madhloom, H. T. et al. [9] used different color space channels to remove the background components. Then the Marker-controlled watershed transform and seeded region growing are utilized to separate the touching cells and the nucleus, respectively. However, this method shows only accurately distinguish between normal

and abnormal cells. In another study, Mohamed, H. et al. [10] built a Gaussian distribution to segment the whole cell from two categories that include similar symptoms diseases. The simple pixel to pixel subtraction was used to separate the nucleus from the cytoplasm. The proposed approach achieved an accuracy of 93% in detecting and classifying acute leukemia types and some subtypes.

3- Methodology

Previously, the mathematical model was developed to give a clear visualization for cells extraction from PB smear images [11], in this study, we proposed a method to segment the acute leukemia and normal cells and their nuclei and cytoplasm from blood smear images. The flowchart of the segmentation scheme is given in Fig. 1.

3-1 Database Description

In order to develop an efficient segmentation method, different staining images are collected from different sources and used in this study. The first collection of images has been taken from Acute Lymphoblastic Leukemia Image Database for Image Processing (ALL-IDB), where the images have been captured using an optical laboratory microscope coupled with a Canon Power Shot G5 camera [12]. While the second one was obtained from the American Society of Hematology (ASH) image bank that provides a high-quality web-based image library for hematological blood images labeled by an expert pathologist [13]. The third set of the collection was pictured from the Shutterstock image bank where American stock photography offers the best quality images [14]. The last set of the collection was gathered from Pathpedia.com that uses as a comprehensive web-based resource to supply quality images for clinical and experimental pathology [15]. The database of this study consists of 132 images of normal and acute leukemia blood smear images labeled by the expert pathologist. In details, it comprises of 50 images for normal patients, 27 images for ALL patients and 55 images for AML patients.

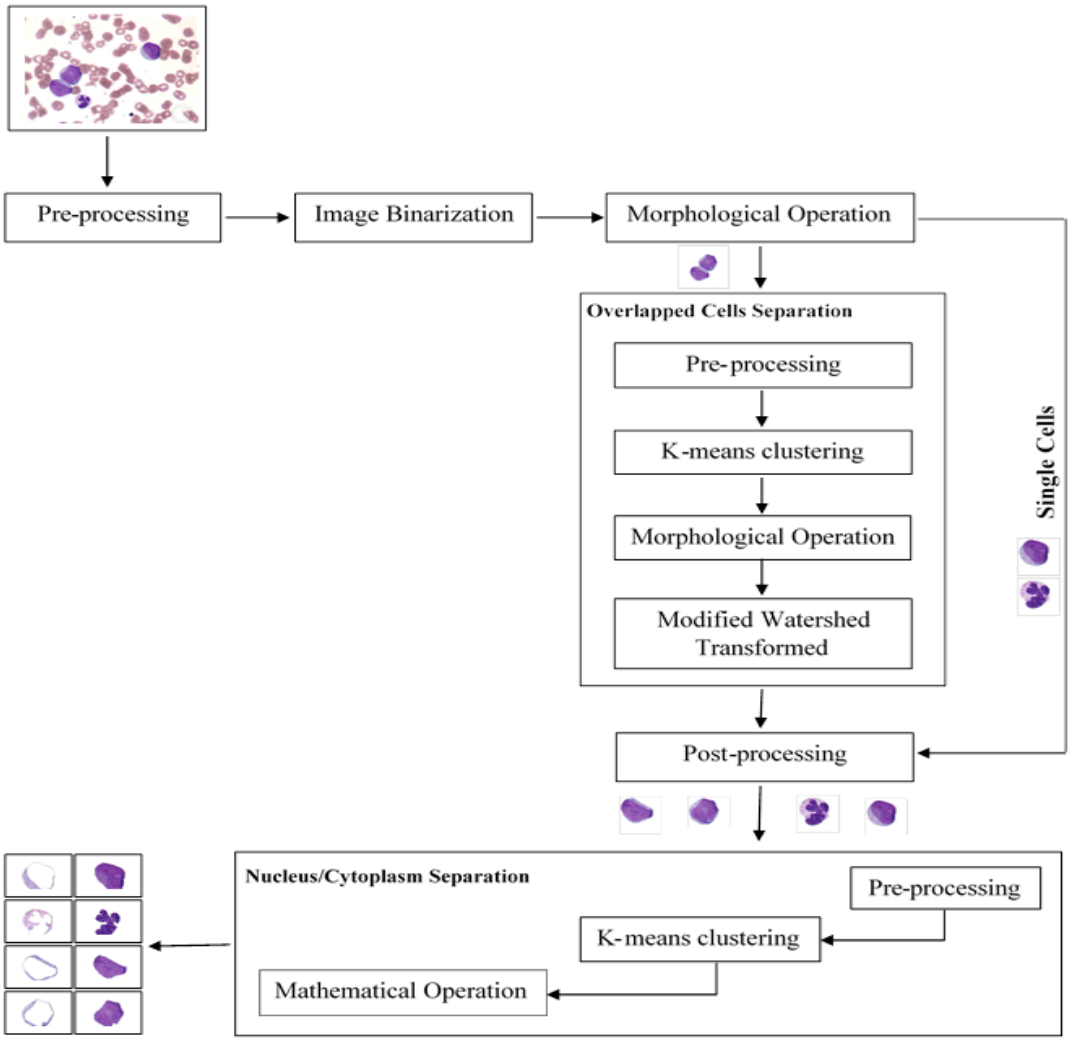

Fig. 1 The flowchart of the segmentation scheme

3-2 Leukocytes Identification

3-2-1 Preprocessing

The PB smear images are usually in RGB color space that may contain some sort of noise, color variation, imbalanced illumination and non – uniformity luminous intensity because of they were obtained from different microscopic settings. Therefore, in this study, the input images were converted to L*a*b* color space Fig. 2(b). L*a*b* color space have three channels one is for Luminance (L*) and the others (a* and b*) are a chromaticity layers. When the color falls along the red-green axis, the a* layer indicates, and when the color falls along the blue-yellow axis, the b* layer indicates. After extracted each L*a*b* color space components Fig. 2(c-e) we have been observed that the WBCs appear more vivid (more details) in b* component while the background

and RBCs (additive noise) almost absent or less in this component, thus b* component is used for cells segmentation [16].

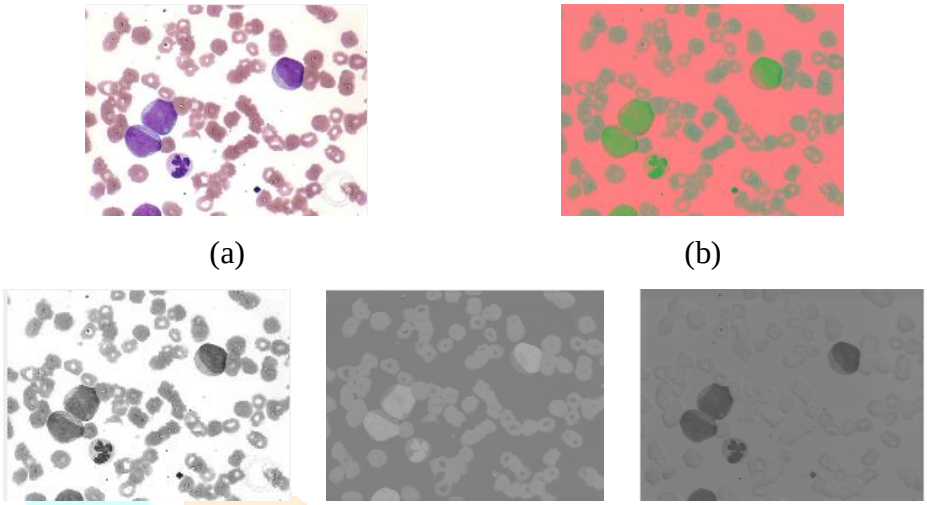

(a) (b)

(c) (d) (e)

Fig. 2 (a) original image, (b) L*a*b* image, (c) L* component, (d) a* component, and (e) b* component

3-2-2 Segmentation

Divided image into regions which have the meaningful information called segmentation and considered as one of the computer vision problems and play an essential rule in the pattern classification. The details of this stage are explained as follow.

3-2-2-1 Image Binarization using Otsu's method

To extract the blast cells that also called a Region of Interest (ROI) from the b* channel (or grayscale image), an automatic threshold calculation (Otsu's method) was performed [17] and the binary image was produced by the following equation

$$\forall(i,j) \in I_{output}, I_{output}(i,j) = \begin{cases} 1 & I(i,j) \geq T \\ 0 & I(i,j) < T \end{cases} \quad (1)$$

, where I_{output} is the binary output image and $I(i,j)$ is the input image. The threshold result is displayed in Fig. 3

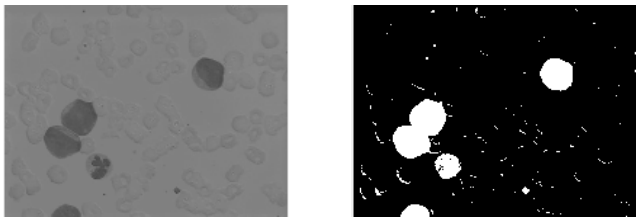

(a) (b)

Fig. 3 (a) b* component, and (b) binary image.

As shown in Fig. 3(b) the binary image may contain some noise that threshold method cannot distinguish it from the background and should be removed. Thus, the morphological operations namely; flood-fill, opening and dilation were used. We started with the flood-fill operation in order to fill the holes of the blast cells. Next, the opening operation was used to eliminate the remaining background and smooth the blast cell surface contours [18]. This is applied by using structure element (SE) with a disk shaped whose radius is 15 pixels. The opening operation can be defined as

$$I \circ SE = (I \ominus SE) \oplus SE \quad (2)$$

, where I is the binary image and SE is the structured element, $\ominus$ is the erosion operation and $\oplus$ is the dilation operation. Fig. 4 displays the binary image after morphological operations.

In addition, the resulted binary image may contain overlapped cells that need an additional treatment in order to get a single cell in each sub-image. Therefore, the following section introduces the process that was done to solve this problem.

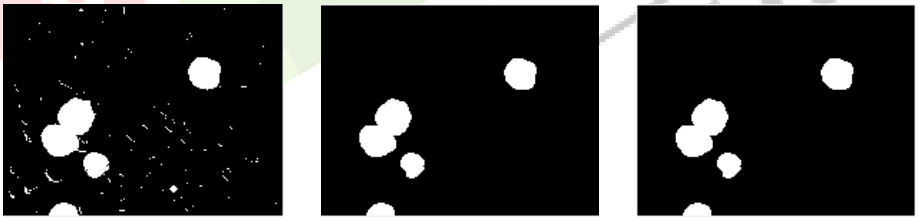

(a) (b) (c)

Fig. 4 (a) binary image, (b) binary image after filling holes, and (c) binary image after opening operation.

3-2-2-2 Identification and Segregation of Overlapped Cells

To extract an individual blast cells, two measures; area and compactness were used to distinguish them from the single cells as described in the equations 3 and 4 [19]. To do that, the area of the overlapped cell was determined to be greater than $7000/factor$ where the value of the $factor$ was selected based on the image dimension.

$$Area = \sum p \quad (3)$$

$$Compactness = Area/(2 * pi * perimeter^2) \quad (4)$$

, where p is the image pixel. In the compactness measure the value of 0.83 for each object was selected to determine the overlapped object [20]. The results are shown in Fig. 5.

3-2-2-2-1 Nucleus segmentation from overlapped cells

To segregate the selected overlapped cells, several methods namely; k-means clustering, watershed segmentation and morphological operation were applied. Since the segmented image should finally display in the RGB color space, the channels a* and b* that contain all color information of the image were chosen for a nucleus segmentation in the following section [21].

3-2-2-2-1-1 K-means Clustering

K-means clustering is an unsupervised learning algorithm that tries to partition the dataset by moving them from one non-overlapped group (cluster) to another until obtained the desired clustering structure [22]. It is applied on the pixels of a* and b* layers which contain all the color information by measures the Euclidean distance among each pixel to another and repeated them 5 times to avoid fall in local minima. The value of k used in cluster is 3 (nuclei, the entire cells and peripheral zone round the cells) Fig. 6(c). Programmatically the mean of each object was determined using the b* layer in the color space and the nuclei that has the minimum mean in b* channel was segmented. Then extracted nuclei cluster was converted to a binary format using the threshold value using the Otsu's method as shown in Fig. 6 (d and e).

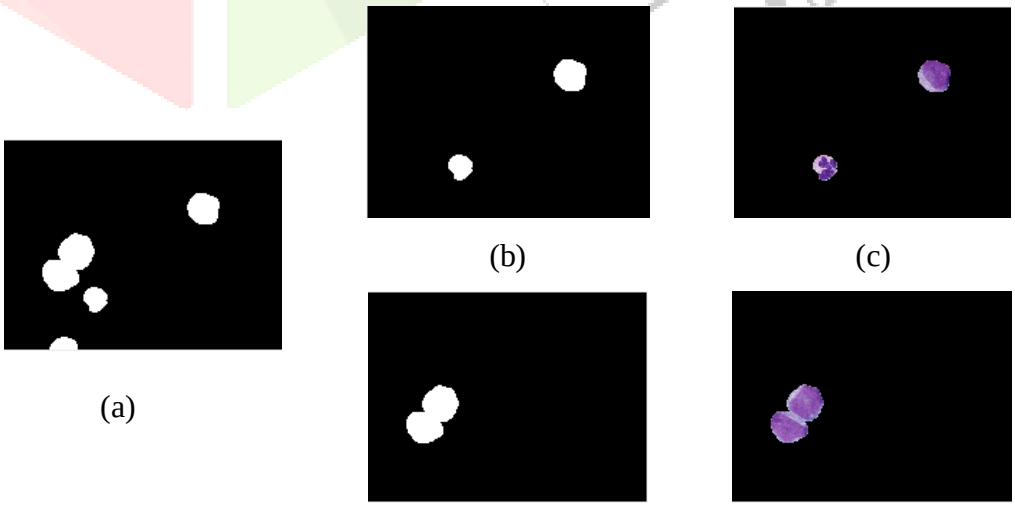

(a) (b) (c) (d) (e)

Fig. 5 (a) binary image, (b) binary image for single cells after removing border touching cells, (c) RGB image for single cells, (d) binary image for grouped cells, and (e) RGB image for grouped cells.

3-2-2-2-1-2 Morphological Operation

In order to delete the artifacts caused by the threshold process in the corresponding binary image some morphological operations were applied. In this case, morphologically open binary image was used to eliminate small objects and smooth the boundaries surrounding the nuclei. Next, the flood fill operation was used to fill the small holes in the image. Finally, the dilation operation was applied to increase the boundaries of nuclei pixels [18]. The result can be seen in Fig. 6 (f - h).

3-2-2-2-1-3 Modified Watershed Transform

To separate the connected nuclei and avoid the over-segmentation problem arising from their sensitive to local minima a modified watershed transform should be applied over the binary image presented in Fig. 6 as follows. First, the Euclidean distance transform was used to calculate the distance from each black pixel to the nearest white pixel. Second, for each blast cell in the PB smear image, Ultimate Eroded Points (UEPs) [23]; the pixels that coincide with local maxima, was used as a marker (catchment basins maxima) [24]. Third, to avoid the over-segmentation the imextendedmin Matlab function was used on the inverse of the inner distance in order to calculate and filter the tiny local minima of the input image and get a marker as a mask [25]. Fourth, the inverse of the distance transform (D1) was then imposed to create a marker as a mask that has only the minima by modifying the intensity of input image using morphological reconstruction. Finally, the watershed transformed was applied on the binary mask image and the results are shown in Fig. 7.

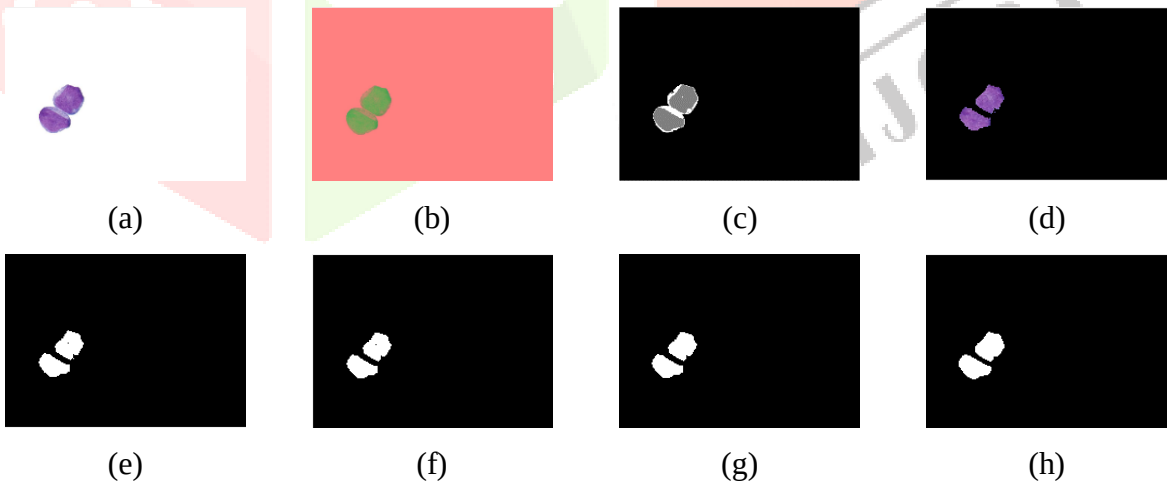

Fig. 6 (a) RGB grouped cells, (b) L*a*b* image, (c) cluster image, (d) nuclei cluster, (e) binary image for nuclei cluster, (f) binary image after opening operation, (g) binary image after filling holes operation, and (h) binary image after dilation operation.

3-2-2-2-2 Cell segmentation for Overlapped cells

After the segregation process of the connected nuclei of overlapped blood cells, another modified watershed transform based on the gradient method was used to separate the overlapped cells as follows. First, the gradient image was obtained by applying the Sobel operator, who can detect the edge of the overlapped blood cells, on the grayscale image. Second, to avoid the over-segmentation problem in this step, the regional maximums of the gradient image were obtained to modify the watershed transform algorithm and eliminate all maximums within the nuclei [25]. Finally, the watershed transform was applied on the output image obtained after the splitted nuclei mask was imposed to it [7]. The result can be shown in Fig. 8.

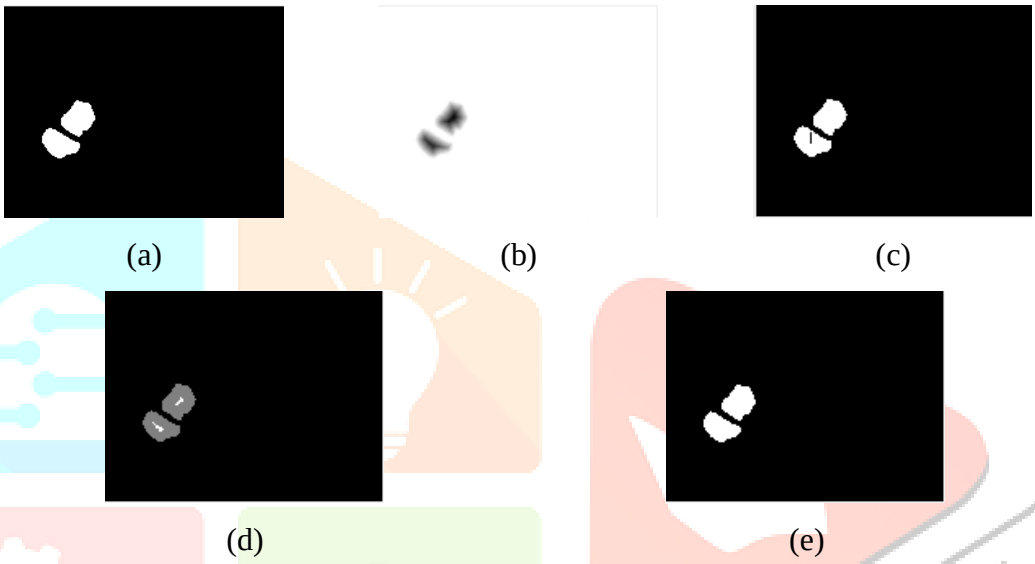

Fig. 7 (a) nuclei binary image, (b) inverse of the distance transform of a, (c) watershed applying on b, (d) markers identification, each of them represent a single nucleus location, and (e) binary image after imposing d on b and applying the watershed.

3-2-2-3 Post-processing

After separating the overlapped cells, the mask of each cell was individually created. However, some of these cells do not have a well-defined border which significantly increases the possibility of wrong diagnosis. Thus, these cells must be deleted.

3-2-2-4 Sub-Imaging

The PB smear images mostly contain more than one blast cell per each image. However, to differentiate between healthy and non-healthy cells and among various acute leukemia subtypes, we need to extract each blast cell into a single sub-image. Thus a crop step using bounding-box and centroid was performed to produce a sub-image for each cell [9].

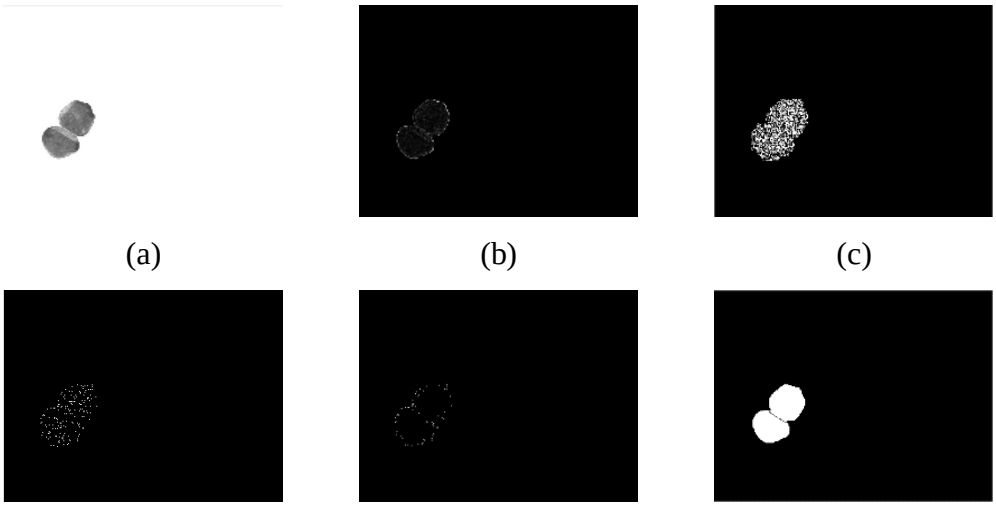

(a) (b) (c)

(d) (e) (f)

Fig. 8 (a) gray scale image, (b) gradient image, (c) watershed applied on b, (d) regional maximum of gradient image, (e) imposing binary image of nuclei splitting mask on d, and (f) watershed output after applying on e.

3-2-2-5 Nucleus / Cytoplasm Separation

In this step, the nucleus of each single blast cell into a single sub-image was separated from the cytoplasm for further analysis by using the k-means clustering algorithm described in section 3-2-2-2-1-1. Next, the cytoplasm was obtained by the pixel to pixel subtraction between the whole cell and its nucleus [10]. Fig. 9 displayed the nucleus/cytoplasm separation of the blast cell into the sub-image.

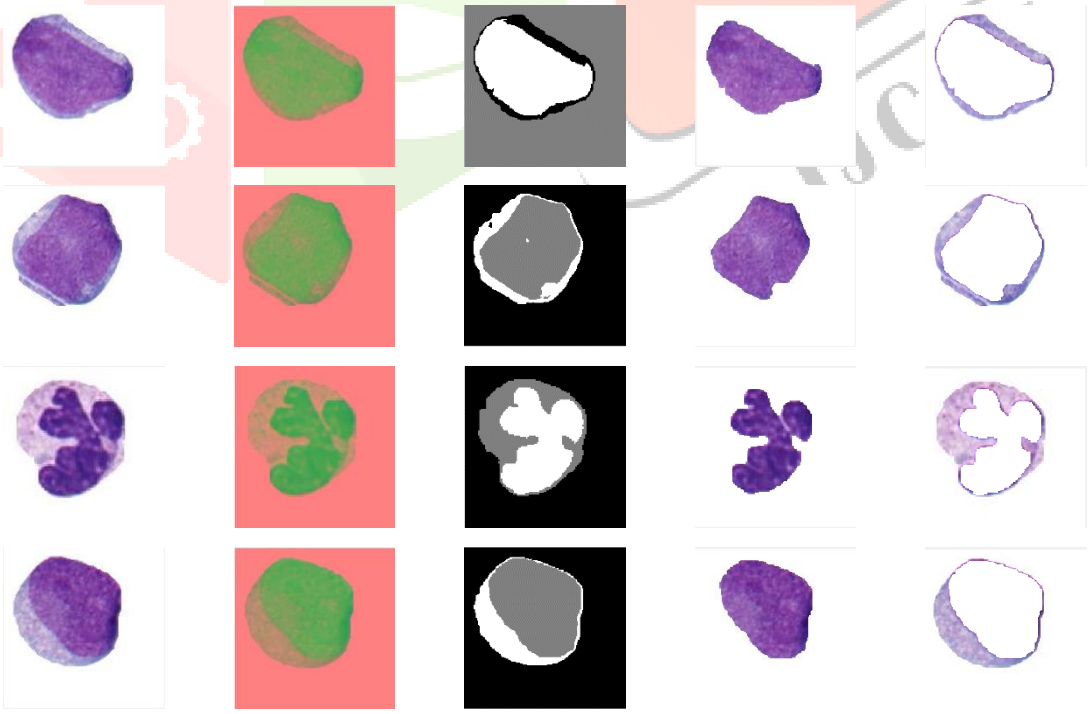

(a) (b) (c) (d) (e)

Fig. 9 (a) cell RGB image, (b) cell L*a*b* image, (c) cell cluster image, (d) cell nucleus, and (e) cell cytoplasm.

4- Results and Discussion

The proposed segmentation method was performed in Intel® Core™ i7-2670 QM CPU@ (2.20 GHz, 8 cores), 8 GRAM runs under windows 7 operating system and the development environment is MATLAB 2017.

4-1 Segmentation Evaluation

In order to measure the performance of the proposed blast cells segmentation algorithm, the ground truth (GT) for each PB smear image have been manually localized and segmented by a hematologist. The performance test of the localization algorithm was evaluated by comparing the percentage of the mis-segmented pixels between the proposed localization algorithm and the ground truth. To do that, three well-known image segmentation evaluation measures were used namely; *Sensitivity*, *Specificity*, and *Accuracy* to evaluate our segmentation method. Hence, to produce a maximum performance rate in terms of the segmented regional size, four terms namely; true positive that represent the foreground pixels (TP_g), true negative that represent the background pixels (TN_g), false positive that represent the missed foreground pixels (FP_g) and false negative that represent the missed background pixels (FN_g) were used. The performance test was conducted over 413 sub-images collected from different sources. The difference between the ground truth and its segmented image was firstly computed for each normal/blast cell subtypes and their respective nuclei separately. Next, the averaged value over ALL subtypes, AML subtypes, acute leukemia types and the normal cells were also calculated. The final evaluation results of normal and each type/subtype blast cells are tabulated in Table I.

Table I The difference between ***ground truth*** and the results of ***our segmentation method*** for all sub-images extracted from the dataset

Cell Type	Cell region			Nucleus region		
	Sens. %	Spec. %	Acc. %	Sens. %	Spec. %	Acc. %
L1	91.70	99.91	99.70	93.24	98.36	96.86
L2	93.36	99.81	99.58	85.40	99.69	94.80
L3	89.37	99.77	99.28	85.98	99.18	95.34
Overall ALL	**91.56**	**99.83**	**99.52**	**87.88**	**99.14**	**95.58**
M0	85.96	91.60	91.54	83.47	89.81	87.92
M1	90.50	97.82	97.42	91.80	96.13	94.92
M2	85.42	92.44	92.15	88.18	91.38	90.35
M3	93.58	99.97	99.83	89.72	97.96	95.98
M4	91.41	96.72	96.44	91.53	94.90	94.12
M5	90.58	96.74	96.62	89.35	94.20	92.82
M7	91.20	99.98	99.70	98.10	97.24	97.41
Overall AML	**89.96**	**96.74**	**96.49**	**90.57**	**94.80**	**93.65**
Overall ALL-AML	**90.20**	**97.44**	**97.17**	**89.70**	**96.20**	**94.27**
Normal	85.14	91.80	91.61	86.67	91.59	90.39
Overall Dataset	**89.25**	**96.37**	**96.12**	**89.01**	**95.14**	**93.38**

4-2 Discussion of results

The performance test of the segmentation was conducted on different dataset sources of ALL subtypes; L1, L2 and L3 by using three segmentation evaluation metrics, namely *Sensitivity*, *Specificity* and *Accuracy*. The ground truth of each blast cell was manually assigned with the help of a domain expert (Gamil Sultan Ahmed Thabet).

The performance test shows excellent segmentation results for 106 sub-images extracted from different PB smear images at average accuracy rate of 99.52% and 95.58% for the blast cells and their nuclei regions, respectively. In case of 216 AML blast cells sub-images extraction, the segmentation achieved an overall average accuracy rate of 96.49% and 93.65% for blast cells and their nuclei regions, respectively. Generally, the performance rate of the AML blast cell's region segmentation was lower than that of the ALL type. This can be attributed to the rate of the missing cells of 3.1% arising from the low variation between the AML cells and its surrounding background components. The lower performance tests in case of M0 subtype compared to other AML subtypes can be assigned to a high rate of missing cells of 8.3% during the segmentation stage. The number of the segmented cells and their associated missed cells are tabulated in the Table II.

In the case of 91 normal cells sub-images extraction, the segmentation achieved an overall average accuracy rate of 91.61% and 90.39 for the normal cell's region and their nuclei. The low efficiency of the segmentation performance tests of the normal cells compared to acute leukemia types can also be attributed to the high rate of missing cells (around 7.1%). In addition, the normal cells in some cases exhibit a reduced size comparing to the other cells which may be considered as artifacts that should be removed through morphologically open binary operation.

Table II Number of segmented and their associated missed cells

Cell type	L1	L2	L3	M0	M1	M2	M3	M4	M5	M7	Normal	Total
No. of segmented cells	31	40	35	22	49	25	31	31	30	28	91	413
No. of missed cells	-	-	-	2	2	1	-	1	1	-	7	14
Total No. of cells	31	40	35	24	51	26	31	32	31	28	98	427
Ratio of missing cells (%)	0	0	0	8.3	3.9	3.8	0	3.1	3.2	0	7.1	3.27

In summary, the proposed algorithm is able to localize the most cells with an overall average segmentation accuracy of 96% and 93 %, for both normal and blast cells and their nuclei regions respectively. Based on these results, the cells (acute leukemia and normal) was used to obtain an accurate diagnosis for acute leukemia from PB smear images [26, 27].

4-3 Comparison with other studies

Due to the lack of the statistical measures in these studies, we only able to do a comparative analysis with the results obtained by Rawat et al. [6]. However, he did not provide any insight of blast cell segmentation. Thus, the comparison is done for nucleus segmentation in terms of sensitivity, specificity and accuracy. From Table III it has been observed that obtained accuracy for the proposed method for the nucleus region was 95.58%, 93.65% and 90.39% for ALL, AML and normal cells, respectively. The results indicate that the proposed method achieved comparable results for ALL and AML nucleus segmentation, however, in the case of AML our study produces this result through the segmentation process for seven AML subtypes compared to three subtypes used by Rawat et al. [6] In case of normal cells the proposed method produced a lower accuracy to nucleus segmentation of 90.39%, this is may be attributed to the high rate of missing cells in our study. In conclusion, the proposed segmentation method provides better performance for the nucleus region segmentation.

Table III Performance comparison between our method and Rawat et al. (2017) method.

Cell type	Nucleus region					
	Our proposed method			Rawat et al. (2017)		
	Senc. %	Spec. %	Acc. %	Senc. %	Spec. %	Acc. %
ALL	87.88	99.14	95.58	86.95	96.54	96.75
AML	90.57	94.80	93.65	84.17	94.10	94.13
Normal	86.67	91.59	90.39	89.24	95.71	97.49

5- Conclusion and future work

Acute leukemia is a heterogeneous malignant disorder of the hematopoietic system that characterized by uncontrolled diffusion of immature blast cells on all ages. Thus, the accurate diagnosis becomes a remarkably issue for the hematologists in order to reduce the mortality rate. This research presents a developed a segmentation methodology for acute leukemia blast cells by using color conversion, threshold algorithm, k–means clustering and mathematical morphological operations in order to produce an accurate and reliable acute leukemia subtype's diagnostic system. To achieve this aim, the blast cell morphology which called the region of interest (ROI) was extracted by converting the RBG PB smear image into L*a*b* color space in order to localize the blast cell. Next, the appeared overlapped cells were segmented into sub – image as a first step of the nucleus and cytoplasm separation. The final segmentation results on 106 ALL sub-images extracted from different sources of PB smear images achieved the best results of 99.52% and 95.58% accuracy. In the case of 216 AML blast cells sub-images, the segmentation showed an overall average accuracy rate of 96.50% and 93.59% for the blast cell regions and their nuclei, respectively. However, these results appeared less accurate of the normal cells of 91.13% and 90.41% and need to develop.

Acknowledgment

The author gives special grateful and thanks to Dr. Gamil Sultan Ahmed Thabet from First Medical Labs, Taiz, who help me to classify the apparent blast cells and select their ground truth in each image.

References

[1] S. H. Katsanis and N. Katsanis, "Molecular genetic testing and the future of clinical genomics," *Nat Rev Genet,* vol. 14, pp. 415-26, Jun 2013.

[2] O. K. Weinberg, R. P. Hasserjian, E. Baraban, C. Y. Ok, J. T. Geyer, J. K. Philip*, et al.*, "Clinical, immunophenotypic, and genomic findings of acute undifferentiated leukemia and comparison to acute myeloid leukemia with minimal differentiation: a study from the bone marrow pathology group," *Modern Pathology,* vol. 32, pp. 1373-1385, 2019.

[3] J. Rodellar, S. Alférez, A. Acevedo, A. Molina, and A. Merino, "Image processing and machine learning in the morphological analysis of blood cells," *International journal of laboratory hematology,* vol. 40, pp. 46-53, 2018.

[4] T. Karthikeyan and N. Poornima, "Microscopic image segmentation using fuzzy c means for leukemia diagnosis," *Leukemia,* vol. 4, pp. 3136-3142, 2017.

[5] A. Nelikanti, "Segmentation and Analysis of Cancer Cells in Blood Samples," *Indian Journal of Computer Science and Engineering (IJCSE).* 2015.

[6] J. Rawat, A. Singh, H. Bhadauria, J. Virmani, and J. S. Devgun, "Computer assisted classification framework for prediction of acute lymphoblastic and acute myeloblastic leukemia," *Biocybernetics and Biomedical Engineering,* vol. 37, pp. 637-654, 2017.

[7] V.-N. Tran, W. Ismail, R. Hassan, and A. Yoshitaka, "An automated method for the nuclei and cytoplasm of Acute Myeloid Leukemia detection in blood smear images," in *2016 World Automation Congress (WAC)*, 2016, pp. 1-6.

[8] L. Putzu, G. Caocci, and C. Di Ruberto, "Leucocyte classification for leukaemia detection using image processing techniques," *Artificial intelligence in medicine,* vol. 62, pp. 179-191, 2014.

[9] H. T. Madhloom, S. A. Kareem, and H. Ariffin, "Computer-aided acute leukemia blast cells segmentation in peripheral blood images," *Journal of Vibroengineering,* vol. 17, pp. 4517-4532, 2015.

[10] H. Mohamed, R. Omar, N. Saeed, A. Essam, N. Ayman, T. Mohiy*, et al.*, "Automated detection of white blood cells cancer diseases," in *2018 First International Workshop on Deep and Representation Learning (IWDRL)*, 2018, pp. 48-54.

[11] A. Najaat, I. Mohammed, and H. Adel, "Mathematical Model of Computer Aided Detection for Acute Leukemia," *International Journal of Computational Engineering Research (IJCER),* vol. 08, pp. 39-50, 2018.

[12] R. D. Labati, V. Piuri, and F. Scotti, "All-IDB: The acute lymphoblastic leukemia image database for image processing," in *Image processing (ICIP), 2011 18th IEEE international conference on*, 2011, pp. 2045-2048.

[13] ASH Image Bank. (2018). *Acute myeloid leukemia*. Available: https://imagebank.hematology.org/

[14] shutterstock. (2019). *Acute myelogenous leukemia images*. Available: https://www.shutterstock.com/search/acute+myelogenous+leukemia

[15] PathPedia. (2019). *Histopathology of blood cells*. Available: https://www.pathpedia.com/education/eatlas/histopathology/blood_cells.aspx

[16] V. S. Rathore, M. S. Kumar, and A. Verma, "Colour based image segmentation using l* a* b* colour space based on genetic algorithm," *International Journal of Emerging Technology and Advanced Engineering,* vol. 2, pp. 156-62, 2012.

[17] S. N. M. Safuan, R. Tomari, W. N. W. Zakaria, and N. Othman, "White blood cell counting analysis of blood smear images using various segmentation strategies," in *AIP Conference Proceedings*, 2017, p. 020018.

[18] D. Chudasama, T. Patel, S. Joshi, and G. I. Prajapati, "Image segmentation using morphological operations," *International Journal of Computer Applications,* vol. 117, 2015.

[19] R. S. Montero and E. Bribiesca, "State of the art of compactness and circularity measures," in *International mathematical forum*, 2009, pp. 1305-1335.

[20] N. Patel and A. Mishra, "Automated leukaemia detection using microscopic images," *Procedia Computer Science,* vol. 58, pp. 635-642, 2015.

[21] K. Patel and R. B. Prajapati, "Segmentation and Classification Techniques of Acute Myeloid Leukemia using Image Processing: A Survey," *International Journal of Scientific Research in Computer Science, Engineering and Information Technology,* vol. 3, pp. 623-628, 2018.

[22] G. Mathur and H. Purohit, "Performance analysis of color image segmentation using k-means clustering algorithm in different color spaces," *IOSR Journal of VLSI and Signal Processing,* vol. 4, pp. 01-04, 2014.

[23] Q.-Z. Ye, "Signed Euclidean Distance Transform Applied to Shape Analysis," in *Issues on Machine Vision*, ed: Springer, 1989, pp. 249-262.

[24] A. Kaur, "Aayushi.: Image segmentation using watershed transform," *Int. J. Soft Comput. Eng.(IJSCE),* vol. 4, pp. 5-8, 2014.

[25] MathWorks. (2020). *Image Processing Toolbox (R2019b)*. Available: https://www.mathworks.com/help/images/index.html

[26] A. Najaat, I. Mohammed, and H. Adel, "GA as a Key Parameter of SVM Parameter Optimization and Feature Selection for Acute Leukemia Diagnosis," *University of Aden Journal OF NATURAL AND APPLIED SCIENCES,* vol. 24, 2020.

[27] A. Najaat, I. Mohammed, and H. Adel, "Acute Leukemia Classification based on Image Processing and Machine Learning Techniques," *International Journal of Innovative Science, Engineering & Technology,* vol. 6, pp. 19-31, 2019.